

# Regional variations in the cellular matrix of the annulus fibrosus of the intervertebral disc

Sabina B. Bruehlmann,<sup>1,2</sup> Jerome B. Rattner,<sup>1,3</sup> John R. Matyas<sup>1,3</sup> and Neil A. Duncan<sup>1,4</sup>

<sup>1</sup>McCaig Centre for Joint Injury and Arthritis Research, <sup>2</sup>Department of Mechanical Engineering, <sup>3</sup>Departments of Cell Biology and Anatomy, and <sup>4</sup>Departments of Civil Engineering and Surgery, University of Calgary, Canada

---

## Abstract

The three-dimensional architecture of cells in the annulus fibrosus was studied by a systematic, histological examination using antibodies to cytoskeletal components, in conjunction with confocal microscopy. Variations in cell shape, arrangement of cellular processes and cytoskeletal architecture were found both within and between the defined zones of the outer and inner annulus. The morphology of three, novel annulus fibrosus cells is described: extended cordlike cells that form an interconnected network at the periphery of the disc; cells with extensive, sinuous processes in the inner region of the annulus fibrosus; and cells with broad, branching processes specific to the interlamellar septae of the outer annulus. The complex, yet seemingly deliberate arrangement of various cell shapes and their processes suggests multiple functional roles. Regional variations in the organization of the actin and vimentin cytoskeletal networks is reported across all regions of the annulus. Most notable is the continuous, strand arrangement of the actin label at the disc's periphery in contrast to its punctate appearance in all other regions. The gap junction protein connexin 43 was found within cells from all regions of the annulus, including those which did not form physical connections with surrounding cells. These observations of the cellular matrix in the healthy intervertebral disc should contribute to a better understanding of site-specific changes in tissue architecture, biochemistry and mechanical properties during degeneration, injury and healing.

**Key words** cell shape; cellular processes; confocal microscopy; cytoskeleton; gap junctions.

## Introduction

The mechanical function of connective tissues depends on the structure of the extracellular matrix, which is maintained by a sparse population of cells. These cells are responsible for co-ordinating the synthesis of the extracellular matrix during connective tissue development, at maturity, and in response to injury. Inter-cellular communication is thought to facilitate and co-ordinate the function of these cells, aided by cell-to-cell connections to span the considerable intervening extracellular matrix. The shape of connective tissue cells has been correlated with the extracellular mechanical

environment (Giori et al. 1993; Matyas, 1994), illustrating linkages between cell phenotype and mechanical load. A rigorous description of morphology therefore serves as a valuable starting point for understanding connective tissue cell physiology. The comprehensive examination of connective tissues by confocal microscopy should provide a complete description of the three-dimensional cellular matrix, which is the morphology, arrangement and interaction of the cells with each other and the surrounding tissue structure.

The functional significance of the cellular matrix is not yet fully understood. In both healing (Lo et al. 2002b) and osteoarthritic tissue (Hellio Le Graverand et al. 2001b) the architecture of the cellular matrix has been altered. In normal connective tissue, regional variations in cell morphology appear to correspond with the local *in situ* mechanical environment of the cell (Ralphs et al. 1998; Hellio Le Graverand et al. 2001a). Moreover, cells in tensile rather than compressive loading environments have cellular processes that extend at some length from

---

### Correspondence

Neil A. Duncan, PhD, Department of Civil Engineering, University of Calgary, 2500 University Drive, NW, Calgary, AB, Canada, T2N 1N4. Tel. (403) 220 8553; fax: (403) 282 7026; e-mail: duncan@ucalgary.ca

Accepted for publication 5 June 2002

the cell body (Lo et al. 2002a). These cellular processes have been identified as prominent features in ligament (Lo et al. 2002b) and tendon cells (McNeilly et al. 1996; Ralphs et al. 1998), as well as in certain regions within the meniscus (Hellio Le Graverand et al. 2001a) and intervertebral disc (Errington et al. 1998). In addition, gap junctions, which serve as conduits for cell-to-cell communication, have been identified within the networks of cellular processes in tendon (McNeilly et al. 1996; Ralphs et al. 1998) and meniscus (Hellio Le Graverand et al. 2001a). This evidence suggests that within connective tissues, the architecture of the extensive, three-dimensional cellular matrix will influence the ability of the cell to sense, maintain and respond to mechanical and chemical changes in the extracellular matrix.

Variations in cell shape (Postacchini et al. 1984; Errington et al. 1998; Hastreiter et al. 2001) and the extent of cell processes (Errington et al. 1998) have been reported among the different regions of the annulus fibrosus. Spherical cells were found in the inner annulus and nucleus pulposus, whereas the cells in the outer annular layers were predominantly elongated, with a smaller population of spherical cells (Errington et al. 1998; Hastreiter et al. 2001). The elongated, or fusiform, cells were orientated parallel to the inclination of the collagen fibres (Postacchini et al. 1984), whose orientation alternates with each successive lamella (Marchand & Ahmed, 1990). Although the cellular processes in the outer annulus were described as long compared to those of the inner annulus, the cellular matrix was reported to be not as extensive as in ligament and tendon (Errington et al. 1998). Recently, gap junctions were identified in cultured disc cells by ultrastructural examination, and by reactivity to antibodies against connexin 43 and 45 in both cultured cells and intact human intervertebral disc (Gruber et al. 2001). However, previous reports have not described the association of gap junctions with the cellular process network, or their regional distribution within the intervertebral disc. Despite the gradual change in biochemical properties across the disc radius (Brickley-Parsons & Glimcher, 1984; Oshima et al. 1993; Best et al. 1994), investigations of cell morphology have compared cells within either two (Errington et al. 1998; Hastreiter et al. 2001) or three (Postacchini et al. 1984; Lotz et al. 1998) preselected radial divisions of the annulus. Consequently, the complete cellular matrix of the annulus fibrosus, and its dependence on radial position, has not yet been elucidated.

The intervertebral disc is a complex, heterogeneous tissue subjected to tensile, compressive and hydrostatic mechanical stresses, with an intricate tissue structure and extracellular matrix to meet these demands. However, the complexities of the *in situ* cellular matrix, whose role it is to maintain the tissue, has not yet been fully characterized. While studies have reported observations of cell shape in the annulus fibrosus in the past (Postacchini et al. 1984; Errington et al. 1998; Hastreiter et al. 2001), incomplete dissection protocols and/or limitations with traditional techniques have underestimated the extent and diversity of the cells. Using a systematic, histological approach this study aimed to determine the three-dimensional architecture of the cellular matrix throughout the annulus fibrosus. The use of antibodies to cytoskeletal proteins, in conjunction with confocal microscopy, identified novel and diverse cell shapes with a complex spatial distribution that illustrated the intricate structure of the intervertebral disc.

## Materials and methods

Twelve bovine tails from 12- to 24-month-old steers were obtained from the abattoir within 2 h of slaughter. The proximal coccygeal disc (CC1–CC2) was exposed, and cleaned of all surrounding ligaments and fascia. The disc was removed by sharp dissection from the adjacent vertebrae and halved. The posterior half was dissected into six pie-shaped sectors (Fig. 1). Three sectors were fixed immediately in fresh 3.7% paraformaldehyde (room temperature, pH 7.4, 2 h); the remaining three were fixed in 100% cold methanol (–20 °C, 2 h) and then washed in phosphate-buffered saline (PBS) (pH 7.4, 4 °C, 2 h). All samples were quick frozen in Tissue Tek OCT® (Sakura Finetek, Torrance, US) and stored at –70 °C until use.

## Cryostat sectioning

The three-dimensional architecture of the cells was studied by sectioning the wedges at 40 µm in three different planes.

1 Tangential sections ( $n = 3$  discs, Fig. 1A) were cut consecutively, in the plane tangential to the lamellae, from the outermost annular layer to the start of the nucleus pulposus. A complete series of sections, taken at intervals of 10 slices (400 µm), was labelled according to one of the protocols detailed below (Methods: Histology).

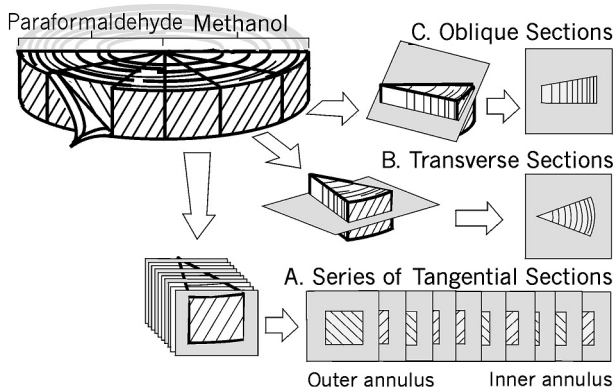


**Fig. 1** The dissection protocol for the posterior half of the coccygeal disc and the orientation of the different cryosectioned planes. A. Series of sections tangential to the lamellar layer at 400- $\mu$ m intervals. B. Sections cut in the transverse plane through the entire thickness of the annulus, from the outer layers to the nucleus. C. Oblique sections, cut at 30° to the transverse plane.

**2** Transverse sections ( $n = 12$  discs, Fig. 1B) spanned the outer annulus to the nucleus pulposus.

**3** Oblique sections ( $n = 6$  discs, Fig. 1C) were cut at 30° to the transverse plane. This enabled a cross-sectional view of the lamellar layers, with the cut surface alternating perpendicular and parallel to the collagen fibre network.

## Histology

A variety of fixation (type, duration, concentration) and staining methods (type, dilution, duration, fixative,

and autofluorescence blocker) were used in preliminary studies to optimize the visualization of the full extent of the cell and its processes. Phalloidin (probe for F-Actin) and antivimentin were chosen for visualization of the cytoskeletal network, anticonnexin 43 was used to identify a gap junction protein, and propidium iodide (PI) was used as a nuclear counterstain. The optimized protocols are summarized in Table 1 and the reagent dilutions are listed in Table 2. In all cases, the sections were washed in PBS following fixation, incubated in 0.5% Triton X100 (5 min) (methanol-fixed sections were first allowed to air dry at room temperature), washed in PBS, incubated in 1% bovine serum albumin (BSA) (Sigma Chemicals Co., St. Louis, MO, USA) (30 min) to reduce autofluorescence and then incubated in the appropriate antibody or stain at 37 °C for the duration indicated in Table 1. After each incubation the specimens were washed twice in PBS. Secondary antibody alone or 0.1% BSA were used as controls.

## Confocal microscopy

Three-dimensional, scanning confocal fluorescent images were collected (Zeiss LSM 510) using a 63 $\times$  1.2NA water-immersion objective lens (Carl Zeiss Inc., Germany) immediately following staining. Settings of laser power and gain were adjusted as required for the particular specimen. Except where otherwise noted,

**Table 1** Summary of labelling protocol

| Structure     | Fixation method                      | 1st Antibody                                 | 2nd Antibody          | Dual label                   |
|---------------|--------------------------------------|--|-----------------------|------------------------------|
| Actin         | paraformaldehyde<br>paraformaldehyde | phalloidin, 3 h<br>phalloidin, 3 h           |                       | PI, 5 min                    |
| Vimentin      | cold methanol                        | antivimentin, 3 h                            | FITC, 2 h             |                              |
| Gap Junctions | cold methanol<br>cold methanol       | anticonnexin 43, 5 h<br>anticonnexin 43, 5 h | FITC, 2 h<br>Cy3, 2 h | PI, 5 min<br>phalloidin, 3 h |

**Table 2** Antibodies and stains

|                      | Product                 | Manufacturer  | [Conc.]     |
|----------------------|-------------------------|---|-------------|
| Primary Antibodies   | anti-vimentin           | Boehringer Mannheim (Laval, QC)                           | 1 : 100     |
|                      | anti-cnexin 43          | Transduction Laboratories (Mississauga, ON)               | 1 : 100     |
| Secondary Antibodies | FITC                    | Sigma Chemicals Co. (St. Louis, MO)                       | 1 : 100     |
|                      | Cy3                     | Jackson ImmunoResearch Laboratories Inc. (West Grove, PA) | 1 : 100     |
| Stains               | Oregon Green phalloidin | Molecular Probes (Oregon, US)                             | 5 $\mu$ M   |
|                      | propidium iodide        | Molecular Probes (Oregon, US)                             | 2.5 $\mu$ M |

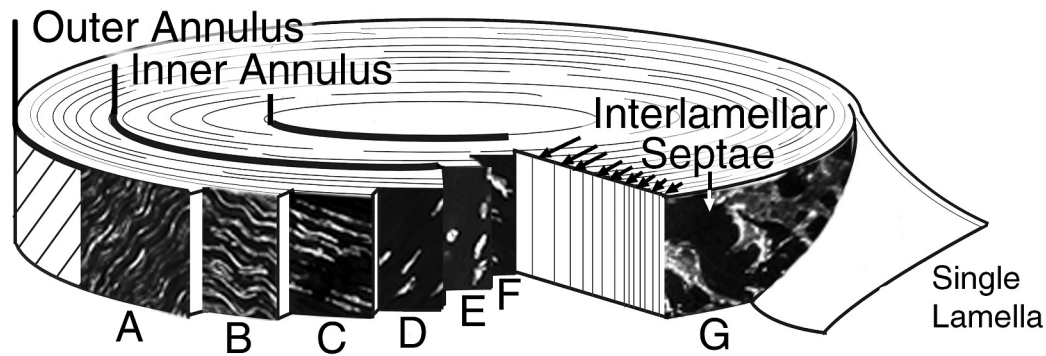


**Fig. 2** Division of the outer and inner annulus zones by identification of cell morphology. The outer annulus is characterized by cells with a fusiform cell body and a gradual transition in process architecture, while the inner annulus consists of cells with a spherical morphology. A–D. Outer Annulus: (A) A dense network of cells with cord-like processes in the longitudinal direction. (B,C) Cells with lateral and reduced length longitudinal processes. (D) Fusiform cells without processes. E,F. Inner Annulus: Cells with extensive, sinuous processes interspersed among spherical cells with at most two short processes. G. Interlamellar septae: a population of disc-shaped cells with a unique process architecture identified between the lamellar layers of the outer annulus.

images were collected as stacks of optical sections ( $z = 1 \mu\text{m}$ ) at  $1024 \times 1024$  resolution with four or eight-line averaging, depending on the background noise, with the pinhole set to one Airy Unit. The images are presented as two-dimensional projections of a three-dimensional stack, created using Zeiss LSM510 software (the specific stack depth is indicated in the caption for each image). The images were processed using Adobe Photoshop Version 5.0.

### Electron microscopy

To validate the confocal observations in specific regions, electron microscopy was performed on sections made in both the oblique and the tangential planes of one disc, as previously described (Hellio Le Graverand et al. 2001a). Sections were examined on a Hitachi H-7000 EM operating at 75 kV.

## Results

### Regional variations in the morphology of lamellar cells

A complex regional variation of cell morphology was found across the annulus fibrosus that can be presented as two regional zones: the outer and inner

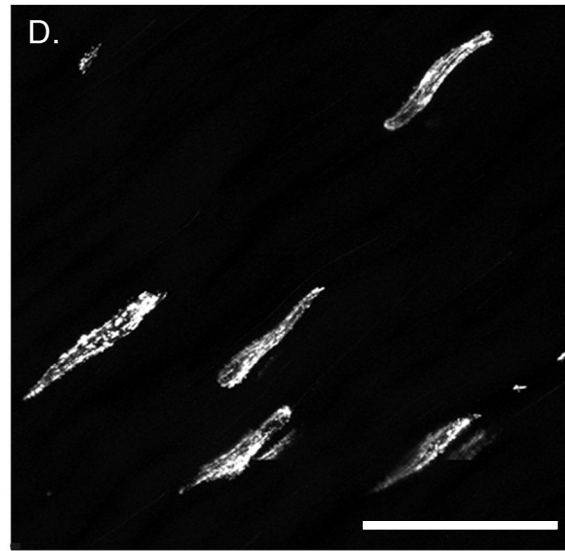
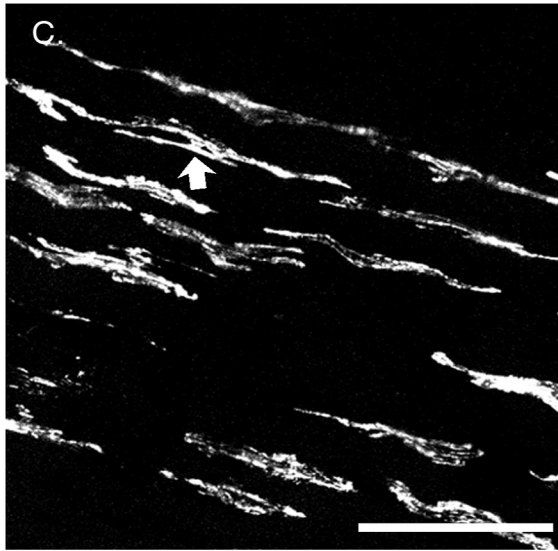
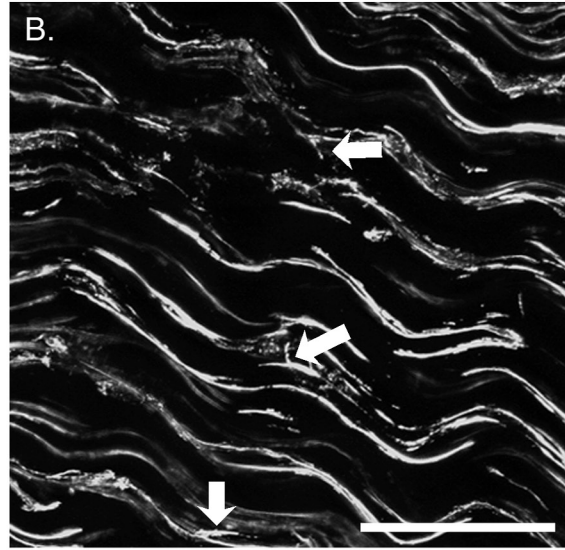
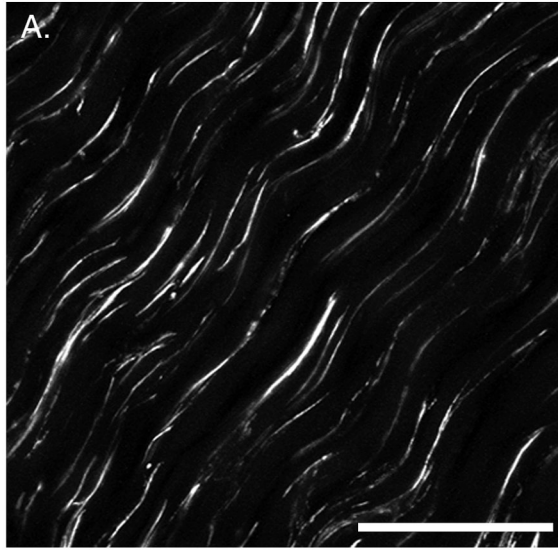
annulus (see Fig. 2). The demarcation between these zones was assigned only after analysis of cell morphology and was not specified *a priori*. Although many complexities exist in the shape and architecture of the cells within each zone, the outer annulus was designated as the region where cells within the layers had a fusiform cell body (Fig. 2A–D), while the inner annulus was the region characterized by spherical cells (Fig. 2E,F). In addition, a distinct cell morphology, which also displayed some regional variation, was identified in the space between the lamellar layers (these are concentric layers of collagen sheets that form the structure of the annulus) (Fig. 2G).

### Outer annulus

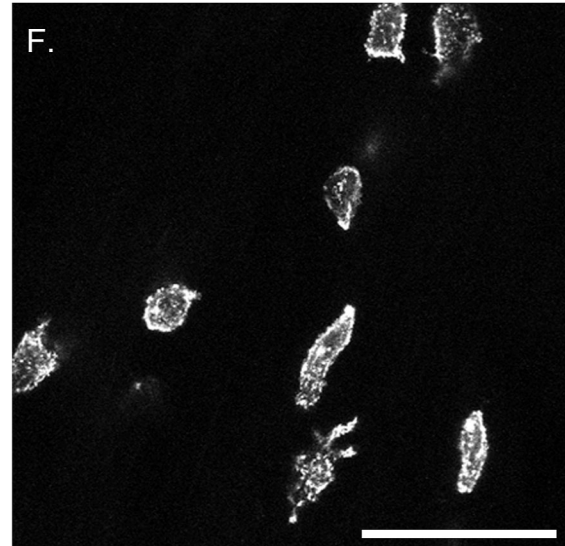
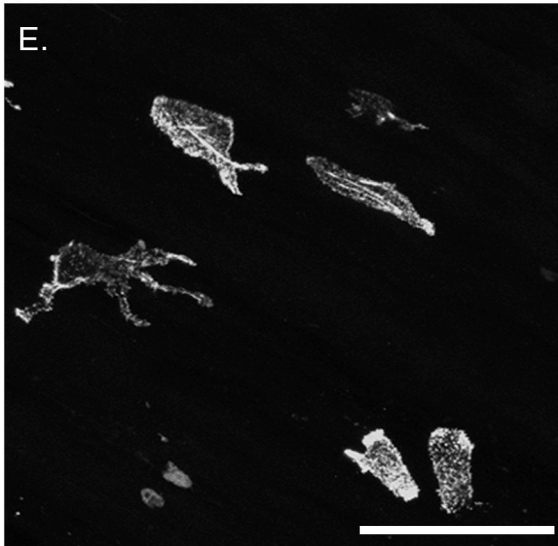
The fusiform shaped cells within the lamellae of the outer annulus were extended along the collagen fibre direction by longitudinal processes that changed gradually with radial position. This was apparent with both actin and vimentin antibody labelling. At the periphery of the disc, the external 20% of the outer annulus zone, the processes were extremely long, thin and uniform along the collagen fibre (longitudinal) direction. The length of these processes, which often exceeded  $60 \mu\text{m}$  from the cell body, could only be

**Fig. 3** Series of two-dimensional projections in the tangential plane of actin-labelled sections demonstrates gradual transition of cell morphology through the thickness of the annulus.  $z_{\text{proj}} = 20 \mu\text{m}$ . Scale bar represents  $50 \mu\text{m}$ . A–D. Outer annulus: (A) Cord-like cells at the periphery. (B) Reduction in the length and increase in the thickness of the longitudinal processes and appearance of some lateral processes (arrows). (C) The longitudinal processes are further reduced in length and isolation of cells is apparent. In addition, lateral processes turn and follow the collagen fibre direction, sometimes bifurcating (arrow). (D) Fusiform-shaped cells with no processes at the border with the inner annulus. E,F. Inner annulus: spherical cells with either short or extensive processes and some elongated cells.

## Outer Annulus



## Inner Annulus



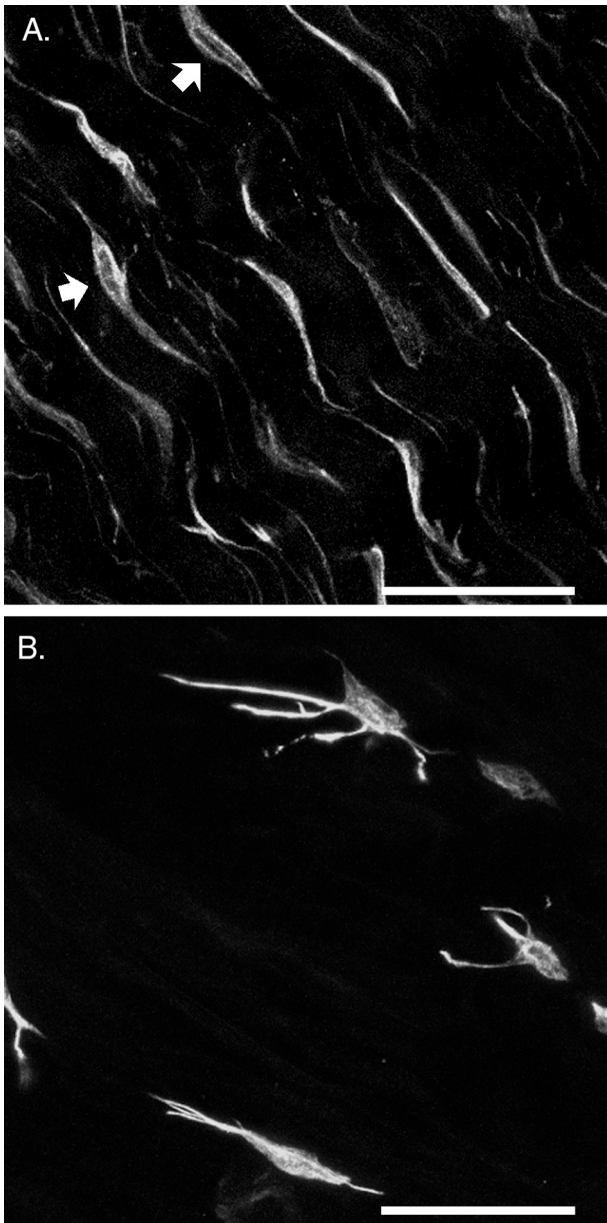


**Fig. 4** Regional differences in cell morphology labelled with antibody to vimentin. Two-dimensional projections:  $z_{\text{proj}} = 15 \mu\text{m}$ . Scale bar represents  $50 \mu\text{m}$ . A. Outer annulus cells (region comparable to Fig. 3A): arrows point to cells where the nucleus outline is visible through the projection. B. Inner annulus cells.

established by three-dimensional stacks of optical sections in the tangential plane (Fig. 3A). Their cordlike appearance and the formation of a continuous network by tip-to-tip contact was most evident with the actin label (Fig. 3A). The fusiform shape of the cell body, on the other hand, was easier to identify when labelled with antivimentin (Fig. 4A). This was followed by a region where the longitudinal processes were

gradually reduced in length and simultaneously increased in thickness with each successive lamella towards the inner annulus. (Fig. 3B,C). Throughout this region, multiple processes were found to extend in parallel along the collagen fibre direction from a single cell; and lateral processes, which extended from the cell body in a direction perpendicular to the collagen fibres, became more numerous with radial depth (arrows, Fig. 3B). Occasionally, longer lateral processes were observed to extend to the bodies of cells in neighbouring rows. If the lateral processes extended beyond this distance, they most often turned to follow the fibre direction, sometimes bifurcating and continuing in opposite directions (arrow, Fig. 3C). By mid-way through the outer annulus it became increasingly difficult to detect physical contact between processes from adjacent cells. Throughout the final 20% of the outer annulus zone, near the border of the inner annulus, the processes had completely disappeared (Fig. 3D). In this region the cells were completely isolated without any apparent physical, intercellular connections.

The lack of lateral processes in the periphery of the outer annulus was confirmed in the transverse plane (Fig. 5) as well as in the oblique plane where the cell network appeared as an array of unconnected points (Fig. 6A). This was also verified by electron microscopy images taken in both the tangential and the oblique planes, where the multitude of small circles from the processes in cross-section were each clearly surrounded by an intact cell membrane (image not shown). The stellate arrangement of the lateral processes in the mid-region of the outer annulus was better viewed in the oblique plane (Fig. 6B).

#### Inner annulus

At least 50% of the radial thickness of the annulus was designated as the inner annulus zone in all specimens observed. The majority of spherical cells in this zone had at most one or two short processes (Fig. 3E,F). However, among these cells were interspersed a population of large bodied cells whose morphology was markedly distinct. These cells were found throughout the inner annulus, although they were more frequent at the border of the nucleus. They had long and impressive processes, which exhibited multiple branching with no directional preference (Fig. 3E). Physical connections were sometimes observed among these cells,

although the processes often appeared to extend in a direction opposite to that of a neighbouring cell. The presence of these cells within layered regions of the annulus, as opposed to the nucleus pulposus, was verified by macroscopic inspection of transverse sections where lamellar layers were clearly visible. These processes were present whether the cell was labelled with antibodies to actin (Fig. 3E) or vimentin (Fig. 4B). Fusiform shaped cells were found mixed among the spherical cells at the boundary of the inner and outer annulus, as well as occasionally (< 2%) throughout the inner annulus.

#### Interlamellar cells

At the interface between the lamellar layers (an area referred to as the interlamellar septae), a distinct population of cells was identified (see Fig. 2). In clear contrast to the fusiform cells within the adjacent layers of the outer annulus, the cell body and nucleus of the interlamellar cells were found to have a flattened, disc-shaped morphology (Fig. 7B). In the plane tangential to the lamellae they appeared round; however, their true disc shape was revealed by three-dimensional reconstructions and observations in the transverse and oblique planes (where, notably, the disc-shaped cells would appear fusiform in cross-section). The positioning of the spherical, interlamellar cells within the septae was established in tangential sections, by observing a change in the orientation of the fusiform cells in the adjacent layers as they followed the alternating direction of the collagen fibres (Fig. 7A). As this alternating orientation was not apparent among the spherical cells within the inner annulus, the existence of interlamellar cells within this region could not be determined.

The arrangement of the cellular processes of the interlamellar cells was distinct. Broad, flat processes with multiple branching sites were found to extend in all directions in a stellate pattern (Fig. 7A) throughout most of the septae of the outer annulus. The network of connecting processes created a thin layer of cells with a lace-like appearance (Fig. 7B), which never appeared to be more than one cell in thickness. The extent of these processes was similar to those of the cells within their adjacent lamellae, and consequently a variation existed across the outer annulus. For example, in contrast to the interlamellar cells already described, the cells found within the interlamellar

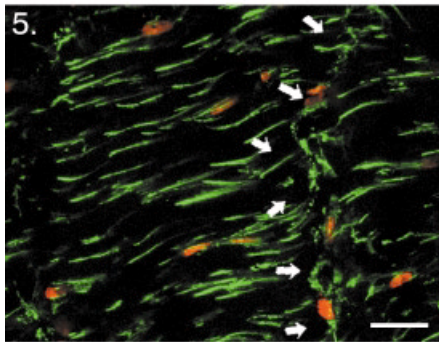
septae of the deepest regions of the outer annulus were devoid of cellular processes (image not shown). Occasionally in the outer annulus, a series of spherical cells crossed the lamella perpendicular to the direction of the collagen fibres (Fig. 5, arrows). Their processes were also large and broad, although they exhibited less branching than the interlamellar cells.

#### Observations of cytoskeletal architecture and connexin 43 distribution

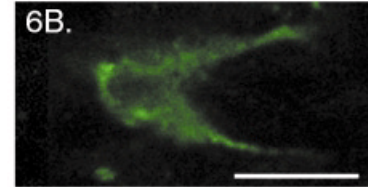
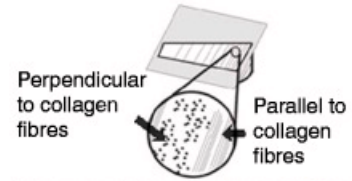
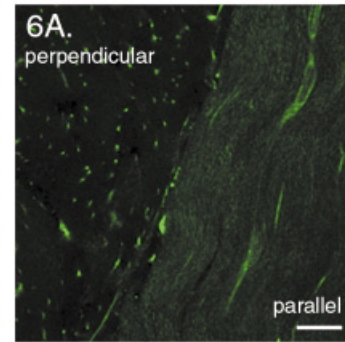
Characteristics of the actin and the vimentin networks were evident as a consequence of the cytoskeletal antibodies used to study the architecture of the cellular matrix in the annulus fibrosus. Vimentin formed a network with a cage-like structure that was consistently observed in cells throughout all regions of the annulus (Fig. 8E,F). It appeared to extend from the nucleus to the cell membrane, and throughout the entire length of the cell processes. In contrast, regional variations were apparent in the organization of the actin network. It appeared as dense, punctate labelling along the cell membrane in all cells of the inner annulus and deep layers of the outer annulus (Fig. 8C,D), as well as within all interlamellar cells (Fig. 7C). This cortical distribution, about both the cell body and the processes, seemed to offer a complete outline of the cell. However, the shape and position of the cell nucleus was not clear. A different organization of the actin network was identified in the periphery of the outer annulus, where the punctate labelling appeared to form continuous strands within the processes. Occasionally, it was possible to track the extent of one of these labelled strands and their extraordinary length could be appreciated (Fig. 8A). Within the cell body, these strands appeared to branch out and surround the nucleus (Fig. 8B), making it difficult to identify the cell body without a nuclear counter stain.

To investigate whether the cells were connected via gap junctions, as demonstrated throughout cellular networks in other connective tissues (McNeilly et al. 1996; Ralphs et al. 1998; Hellio Le Graverand et al. 2001a), the sections were labelled for the gap junction protein connexin 43. Labelling appeared throughout every region of the annulus. Numerous sites of labelling were observed along the long, thin processes of the periphery of the outer annulus (Fig. 9A), highlighting their shape, as well as within the cell body (Fig. 9B). Among the isolated cells of the outer annulus and

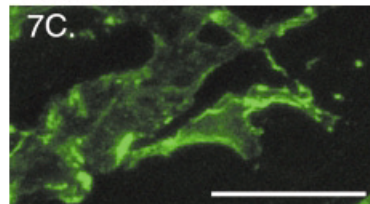
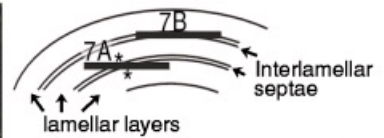
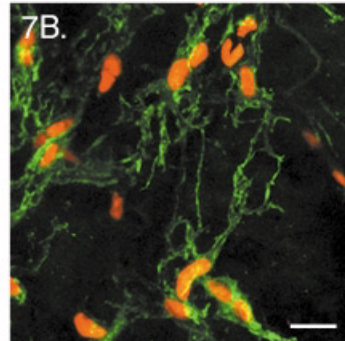
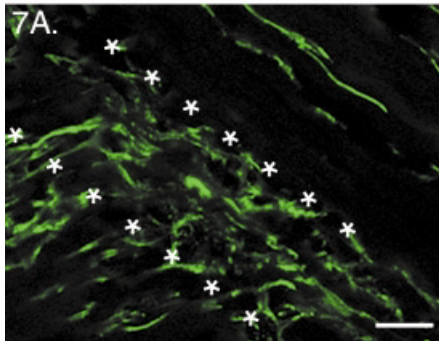
### Transverse Section



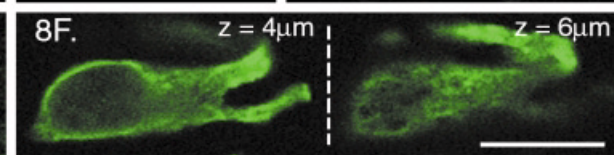
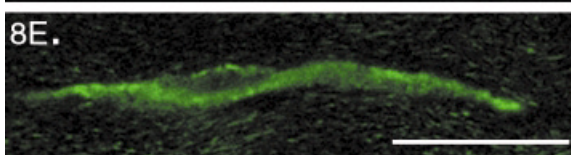
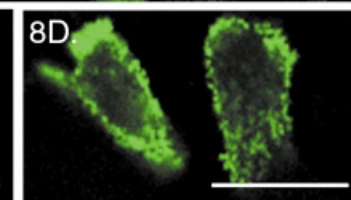
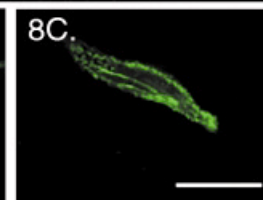
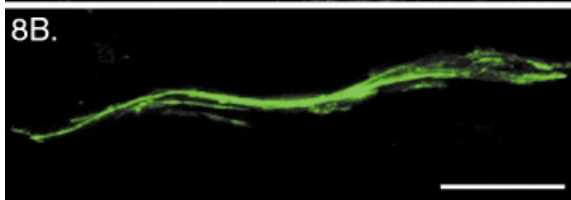
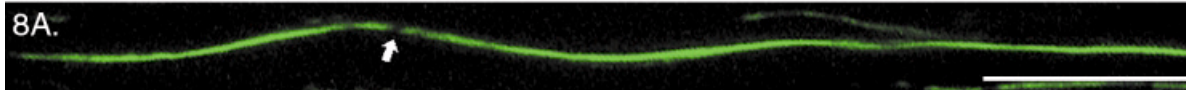
### Oblique Sections



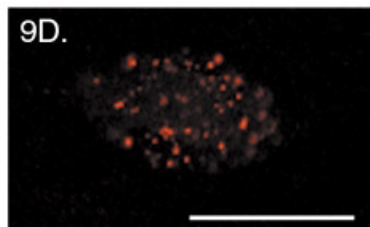
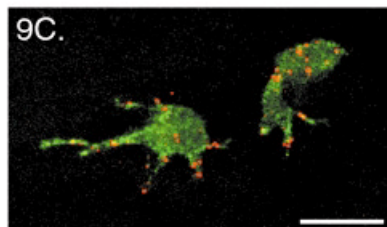
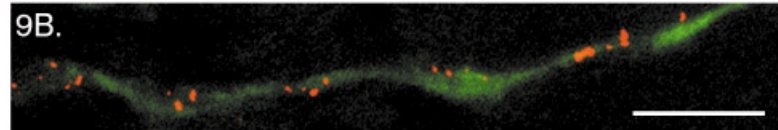
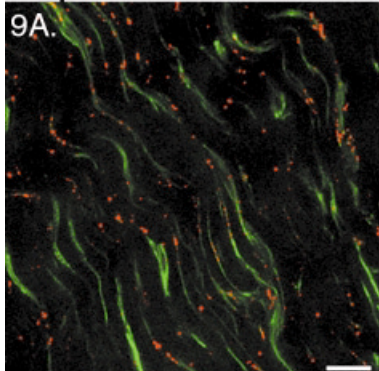
### Interlamellar Cells



### Cytoarchitecture



### Expression of Connexin 43





throughout the inner annulus, connexin 43 was also expressed. It could be found at the tip of their processes even when these cells appeared to be separated from any other cells by considerable extracellular matrix (Fig. 9C). There was often very intense and dense labelling along the membrane of the cell body, with some staining also appearing within the central portion of the cell (Fig. 9C,D).

## Discussion

The aim of this study was to determine the three-dimensional architecture of the cells throughout the bovine annulus fibrosus. By systematic examination, using antibodies to cytoskeletal proteins in conjunction with confocal microscopy, an elaborate cellular matrix with regional variations in cell shape, arrangement of cellular processes and cytoskeletal architecture was revealed.

This study is consistent with earlier reports of cell body shape in the intervertebral disc (Postacchini et al. 1984; Errington et al. 1998; Hastreiter et al. 2001); however, the description of the extent and architecture of the cellular processes of the present study illustrates a significantly more diverse and complex cellular

matrix. These differences are most attributable to the inherent limitations of traditional histological techniques, and incomplete sampling protocols (e.g. investigations of only a single orientation without consideration of radial position). In addition, the present study enabled a more direct comparison among regions by the consistent use of cytoskeletal labels across the radius of the annulus. The result is a comprehensive model of the cellular matrix in the annulus fibrosus (Fig. 2), which includes three novel morphological descriptions. Knowledge of the variations in the cellular matrix may prove to be central to biochemical and mechanical *in vitro* investigations of cell behaviour and phenotype.

At the periphery of the outer annulus, the cells formed a network that was more extensive than previously reported, with characteristics similar to the cellular matrix reported in tendon and ligament (McNeilly et al. 1996; Ralphs et al. 1998, 2002; Lo et al. 2002b). The second novel cell morphology was identified among the spherical cells of the inner annulus. These cells had extensive sinuous processes, and were similar to cells that had been previously reported only in the nucleus pulposus (Errington et al. 1998). Finally, cells identified

**Fig. 5** Two-dimensional projection in the transverse plane:  $z_{\text{proj}} = 10 \mu\text{m}$ . Outer annular cells stained with actin phalloidin (green) and a nuclear counterstain (propidium iodide: red). Cord-like processes appear short as only their tips are visible as they descend into the tissue at a  $30^\circ$  angle to this plane. Arrows indicate a series of cells with broad processes that traverse the thickness of a lamella. Scale bar represents  $20 \mu\text{m}$ .

**Fig. 6** Single optical section in the oblique plane showing regional variations in lateral processes, labelled with antibody to vimentin:  $z_{\text{proj}} = 1 \mu\text{m}$ . Scale bar represents  $20 \mu\text{m}$ . A. A section cut at  $30^\circ$  to the transverse plane in the periphery of the outer annulus (refer to accompanying diagram). The cells that are cut perpendicular to their longitudinal axis appear as an array of points and demonstrate the lack of lateral projections in this region. B. Cross-section of a cell in the mid-region of the outer annulus where lateral processes have become more prominent.

**Fig. 7** Cells from the interlamellar septae of the outer annulus. Scale bar represents  $20 \mu\text{m}$ . A. Two-dimensional projection ( $z_{\text{proj}} = 20 \mu\text{m}$ ) of a tangential plane at the intersection of two layers (refer to diagram) labelled with antibody to vimentin. The stellate cells, on the diagonal between the \* are the interlamellar cells. B. Two-dimensional projection in the tangential plane ( $z_{\text{proj}} = 5 \mu\text{m}$ ) of interlamellar cells, labelled with actin, depicting the multiple branching and interconnectedness of their broad processes. C. Single optical section ( $z_{\text{proj}} = 1 \mu\text{m}$ ) of an interlamellar cell process showing the cortical and punctate organization of the actin staining.

**Fig. 8** Difference between vimentin and actin cytoskeletal architecture. Scale bar represents  $20 \mu\text{m}$ . A. Actin, periphery of the outer annulus: two-dimensional projection of the cord-like processes, possibly two cells coming together in a tip to tip junction (arrow).  $z_{\text{proj}} = 15 \mu\text{m}$ . B. Actin, mid-region of the outer annulus: single optical section ( $z_{\text{proj}} = 1 \mu\text{m}$ ) depicting the strands of actin filaments in the cell body. C. Actin, inner annulus: a single optical section ( $z_{\text{proj}} = 1 \mu\text{m}$ ) through an elongated cell with punctate and cortical labelling of the actin networks. D. Actin, inner annulus: single optical sections ( $z_{\text{proj}} = 1 \mu\text{m}$ ) through two cells. E. Vimentin, outer annulus: two-dimensional projection ( $z_{\text{proj}} = 5 \mu\text{m}$ ) showing the cage-like appearance of the vimentin structure both within the cell body and along the processes. F. Vimentin, inner annulus: single optical sections ( $z_{\text{proj}} = 1 \mu\text{m}$ ) at two depths within the same cell.  $z = 4 \mu\text{m}$ : clear outline of nucleus;  $z = 6 \mu\text{m}$ : cage-like appearance of the cytoskeletal network.

**Fig. 9** Dual-labelled sections showing the distribution of connexin 43 expression: actin phalloidin (green) and connexin 43 (red). Scale bar represents  $20 \mu\text{m}$ . A. Two-dimensional projection in the tangential plane ( $z_{\text{proj}} = 20 \mu\text{m}$ ) of the outer annulus demonstrating the distribution of connexin 43 along the longitudinal processes. B. Two-dimensional projection ( $z_{\text{proj}} = 10 \mu\text{m}$ ) of a string of outer annulus cells in the tangential plane, with connexin 43 label present at both the cell body and at the junction between the two processes. C. Two-dimensional projection ( $z_{\text{proj}} = 15 \mu\text{m}$ ) of inner annulus cells, connexin 43 is found both within the cell body and along the cell processes. D. Single optical section ( $z_{\text{proj}} = 1 \mu\text{m}$ ) through a spherical cell of the inner annulus, showing multiple sites of connexin 43 labelling both at the cell membrane and within the body (without actin labelling).

previously in the outer annulus of human (Hastreiter et al. 2001) and bovine disc (Errington et al. 1998) as spherical were found to be disc-shaped with a unique cell process architecture and localized specifically within the interlamellar septae.

The elaborate, sheet-like network of broad, branching processes of the interlamellar cells is similar to the recently described cellular matrix of the endoligament, which surrounds the fascicles within the ligament (Lo et al. 2002a). The interlamellar septae are rarely recognized as a feature of the annulus fibrosus; despite having a biochemical composition that is in stark contrast to that of the adjacent lamellar layers. For instance, the interlamellar septae contain proteoglycan aggregates, with water imbibing properties similar to those found within the nucleus of the disc; while the lamellar layers are comprised of proteoglycan monomers which interact with, and modulate the behaviour of the collagen fibrils (Ortolani et al. 1988). The amorphous structure of the collagen and elastin fibres within the septae (Postacchini et al. 1984) resembles their organization within the nucleus (Humzah & Soames, 1988). This difference between the biochemical environments suggests that the interlamellar cells may be a different cell phenotype from the cells within the lamellar layers. The maintenance of such contrasting environments by morphologically distinct cells may provide insight into the dynamic relationship between cell and tissue phenotype. It is also of importance due to the increase in septae width observed with age (Postacchini et al. 1984), and the sudden increase in the number of spherical cells and loss of lamellar structure that was observed in an experimental model of degenerative disc disease (Lotz et al. 1998).

Cellular processes were found to be an even more significant feature of intervertebral disc cells than previously reported (Errington et al. 1998). They are thought to be characteristic of tensile bearing tissues (Lo et al. 2002a) and have demonstrated the ability to withdraw upon the removal of a tensile load in culture (Baschong et al. 1997). However, in the annulus fibrosus long cellular processes were also found to be present within the inner region, which is subjected to compressive stresses (Shirazi-Adl et al. 1984; Adams et al. 1996). It is possible that in the intervertebral disc, the architecture of the cellular processes is a function of several factors. The long cord-like processes of the outer annulus are ideal structures for sensing the tensile loads experienced by this region. Meanwhile,

the reappearance of processes in the compressive environment of the inner annulus and nucleus may be to assist the inadequate nutritional pathways (Maroudas et al. 1975; Horner & Urban, 2001), or the maintenance of remote extracellular matrix due to the decreased cell density (Hastreiter et al. 2001).

The interconnected network of cell processes observed in other connective tissues (McNeilly et al. 1996; Ralphs et al. 1998; Hellio Le Graverand et al. 2001a) is hypothesized to facilitate intercellular communication. In the present study, such a network was only observed in the periphery of the outer annulus fibrosus. Yet, expression of connexin 43, a gap junctional protein that assembles into a hemichannel, appeared throughout the annulus. This is in contrast to studies done in tendon (McNeilly et al. 1996) and meniscus (Hellio Le Graverand et al. 2001a), where connexin 43 was expressed only in tensile environments at sites of contact between processes. No expression was found among spherical cells in fibrocartilage regions of tendon (Ralphs et al. 1998). Even though connexin 43 is commonly used to investigate the possibility of intercellular communication pathways, hemichannels must be located on the plasma membranes of two opposing cells to form a functional gap junction. While the possibility exists that the expression of connexin 43 labelling within unconnected cells has no functional significance, non-junctional hemichannels have demonstrated other functional roles that include the ability to regulate cell volume in an isosmotic environment (Quist et al. 2000).

The punctate labelling and cortical concentration of the actin network among cells of the inner and deeper outer annulus regions is similar to that described for chondrocytes of articular cartilage (Durrant et al. 1999; Idowu et al. 2000; Langelier et al. 2000), as well as cultured outer annulus cells (Guilak et al. 1999). This same cortical organization was seen to extend along the processes as well. The seemingly continuous strands of actin labelling within the processes of the cord-like cells of the outer annulus are similar to those recently described in tendon, where the additional presence of tropomyosin label identified them as actin stress fibres (Ralphs et al. 2002). The regional contrast in cytoskeletal structure may be a reflection of the different mechanical loads experienced by the cells *in situ*. It may also explain the difference in mechanical properties that was measured for inner and outer annulus cells in culture (Guilak et al. 1999). While the presence of smooth muscle actin in human disc (Hastreiter et al.

2001) and actin stress fibres in the discs of developing neonatal rats (Hayes et al. 1999) have been reported, this study is the first report on the *in situ* organization of cytoskeletal networks within the cells of the intervertebral disc. For vimentin, although zonal variations of intensity have been reported, albeit conflicting, in articular cartilage (Durrant et al. 1999; Langelier et al. 2000) and tendon (Ralphs et al. 1991), its tight, cage-like structure was consistent throughout all regions of the intervertebral disc. This organization of the vimentin is characteristic of articular chondrocytes (Langelier et al. 2000) and cells of the meniscus (Hellio Le Graverand et al. 2001a), where it was observed to extend into the processes. It may be a mechanism for transduction of mechanical deformation from cell membrane to nucleus; a phenomenon that has been observed in chondrocytes (Guilak, 1995; Lee et al. 2000).

The correlation of cell shape and prevailing tissue stress has been reported in a number of connective tissues (Giori et al. 1993; Matyas et al. 1994; Matyas, 1994; Duncan et al. 1996; Ralphs et al. 1998). The biochemical composition of the intervertebral disc varies from the outer to the inner annulus (Eyre & Muir, 1976; Brickley-Parsons & Glimcher, 1984; Best et al. 1994), which has been specifically verified with the bovine coccygeal disc (Oshima et al. 1993). Similarly, the mechanical environment varies radially through the annulus (Shah et al. 1978; Shirazi-Adl et al. 1984; Adams et al. 1996; Lotz et al. 1998). The steady increase in compressive stress with radial depth in the outer annulus (Adams et al. 1996) corresponds with the progressive decrease in longitudinal process length and increase in cell body width among the cells of this region. This is followed by a centre region of significant hydrostatic stress, which overlaps the anatomical inner annulus (Adams et al. 1996; Lotz et al. 1998). The hydrostatic region is coincident with the portion of inner annulus where the clusters of nucleus-like cells were found. This close correlation between cell shape and tissue stress suggests that changes in cell morphology will accompany, and possibly predict, alterations to tissue stress that have been observed with endplate fracture (Adams et al. 2000), age and degeneration (Adams et al. 1996; Lotz et al. 1998).

The extensive cell matrix observed in this study was not thought to be an artefact of fixation, as several different fixatives were used in optimizing the protocol for each label and no discrepancies were noted. Electron microscopy was used specifically to verify

the existence of the long, cord-like cells in the outer annulus. However, the extent and three-dimensional arrangement of the cellular matrix was not realized with this technique. Several fluorescent labelling methods were also investigated, including live cell cytoplasmic stains (CMFDA, CFDA, SE, Calcein: Molecular Probes, OR, USA). However, it was noted that processes generally appeared thinner and less extensive with live cell stains. The chosen method, using antibodies to cytoskeletal proteins, has been used in a variety of other tissues for similar morphological examinations (Errington et al. 1998; Hellio Le Graverand et al. 2001a,b; Lo et al. 2002a,b). The noticeable crimp pattern exhibited by the cells, particularly those of the outer annulus, was shown to be an artefact of the preparation, created by the release of tension in the collagen fibres. In preliminary studies, it was found that the crimp was greatly reduced by sectioning a disc that had been frozen with the vertebral bodies intact. However, this method was not feasible for this study because the decreased fixation rate that occurred adversely affected the preservation of cell morphology. Additionally, when the specimens were removed from the vertebral bodies, swelling likely occurred. This could, potentially, have increased the width of the interlamellar septae, consequently allowing the cells to be more easily seen. However, swelling should not have caused only a two-dimensional shape change (resulting in a disc-shaped cell), nor should it have consistently shifted cells from within the lamellae to the interlamellar septae. Therefore, their unique morphology is not believed to be an artefact.

This study has presented a unique model of the cellular matrix across the annulus fibrosus of the intervertebral disc (summarized in Fig. 2). An appreciation of regional distinctions in the extent and morphology of the cellular matrix has implications for the mechanisms of mechanotransduction, nutritional pathways and energy requirements of the cells of the intervertebral disc. Further, the observations suggest that the absence of processes in cultured cells is potentially problematic for investigations of both cell physiology and mechanical properties. It is believed that this knowledge of the regional variations of cell morphology in the healthy intervertebral disc will contribute to a better understanding of site-specific changes in tissue biochemistry and mechanical properties during degeneration, injury, and healing.

## Acknowledgments

We would like to acknowledge the financial support of the Whitaker Foundation (Grant # RG-99-0225) and the Canadian Institutes of Health Research (Grant # MOP-42368). S.B.B. is supported by a studentship from the National Science and Engineering Research Council; J.R.M. is a senior scholar of The Arthritis Society; N.A.D. is supported by the Canada Research Chairs programme. We would like to thank Leona Barclay for preparation of the electron microscopy sections.

## References

- Adams MA, McNally DS, Dolan P (1996) 'Stress' distributions inside intervertebral discs. The effects of age and degeneration. *J. Bone Joint Surg. Br.* **78**, 965–972.
- Adams MA, Freeman BJ, Morrison HP, Nelson IW, Dolan P (2000) Mechanical initiation of intervertebral disc degeneration. *Spine* **25**, 1625–1636.
- Baschong W, Sutterlin R, Aebi U (1997) Punch-wounded, fibroblast populated collagen matrices: a novel approach for studying cytoskeletal changes in three dimensions by confocal laser scanning microscopy. *Eur. J. Cell Biol.* **72**, 189–201.
- Best BA, Guilak F, Setton LA, Zhu W, Saed-Nejad F, Ratcliffe A, et al. (1994) Compressive mechanical properties of the human annulus fibrosus and their relationship to biochemical composition. *Spine* **19**, 212–221.
- Brickley-Parsons D, Glimcher MJ (1984) Is the chemistry of collagen in intervertebral discs an expression of Wolff's Law? A study of the human lumbar spine. *Spine* **9**, 148–163.
- Duncan NA, Liebenberg E, Mathews CHE, Lotz JC (1996) *The Distribution of Mechanical Stress and Cellular Phenotype Are Correlated in the Lumbar Disc*. Proceedings of the 23rd Annual Meeting of the International Society for the Study of the Lumbar Spine, Burlington, p. 21.
- Durrant LA, Archer CW, Benjamin M, Ralphs JR (1999) Organisation of the chondrocyte cytoskeleton and its response to changing mechanical conditions in organ culture. *J. Anat.* **194**, 343–353.
- Errington RJ, Puustjarvi K, White IR, Roberts S, Urban JP (1998) Characterisation of cytoplasm-filled processes in cells of the intervertebral disc. *J. Anat.* **192**, 369–378.
- Eyre DR, Muir H (1976) Types I and II collagens in intervertebral disc. Interchanging radial distributions in annulus fibrosus. *Biochem. J.* **157**, 267–270.
- Giori NJ, Beaupre GS, Carter DR (1993) Cellular shape and pressure may mediate mechanical control of tissue composition in tendons. *J. Orthop. Res.* **11**, 581–591.
- Gruber HE, Ma D, Hanley EN Jr, Ingram J, Yamaguchi DT (2001) Morphologic and molecular evidence for gap junctions and connexin 43 and 45 expression in annulus fibrosus cells from the human intervertebral disc. *J. Orthop. Res.* **19**, 985–989.
- Guilak F (1995) Compression-induced changes in the shape and volume of the chondrocyte nucleus. *J. Biomech.* **28**, 1529–1541.
- Guilak F, Ting-Beall HP, Baer AE, Trickey WR, Erickson GR, Setton LA (1999) Viscoelastic properties of intervertebral disc cells. Identification of two biomechanically distinct cell populations. *Spine* **24**, 2475–2483.
- Hastreiter D, Ozuna RM, Spector M (2001) Regional variations in certain cellular characteristics in human lumbar intervertebral discs, including the presence of alpha-smooth muscle actin. *J. Orthop. Res.* **19**, 597–604.
- Hayes AJ, Benjamin M, Ralphs JR (1999) Role of actin stress fibres in the development of the intervertebral disc: cytoskeletal control of extracellular matrix assembly. *Dev. Dyn.* **215**, 179–189.
- Hellio Le Graverand MP, Ou Y, Schield-Yee T, Barclay L, Hart D, Natsume T, et al. (2001a) The cells of the rabbit meniscus: their arrangement, interrelationship, morphological variations and cytoarchitecture. *J. Anat.* **198**, 525–535.
- Hellio Le Graverand MP, Sciore P, Eggerer J, Rattner JP, Vignon E, Barclay L, et al. (2001b) Formation and phenotype of cell clusters in osteoarthritic meniscus. *Arthritis Rheum.* **44**, 1808–1818.
- Horner HA, Urban JP (2001) 2001 Volvo Award Winner in Basic Science Studies: Effect of nutrient supply on the viability of cells from the nucleus pulposus of the intervertebral disc. *Spine* **26**, 2543–2549.
- Humzah MD, Soames RW (1988) Human intervertebral disc: structure and function. *Anat. Rec.* **220**, 337–356.
- Idowu BD, Knight MM, Bader DL, Lee DA (2000) Confocal analysis of cytoskeletal organisation within isolated chondrocyte sub-populations cultured in agarose. *Histochem. J.* **32**, 165–174.
- Langelier E, Suetterlin R, Hoemann CD, Aebi U, Buschmann MD (2000) The chondrocyte cytoskeleton in mature articular cartilage: structure and distribution of actin, tubulin, and vimentin filaments. *J. Histochem. Cytochem.* **48**, 1307–1320.
- Lee DA, Knight MM, Bolton JF, Idowu BD, Kayser MV, Bader DL (2000) Chondrocyte deformation within compressed agarose constructs at the cellular and sub-cellular levels. *J. Biomech.* **33**, 81–95.
- Lo IK, Chi S, Ivie T, Frank CB, Rattner JB (2002a) The Cellular matrix: a feature of tensile bearing dense soft connective tissues. *Histol. Histopathol.* **17**, 523–537.
- Lo IK, Ou Y, Rattner JP, Hart DA, Marchuk LL, Frank CB, et al. (2002b) The cellular networks of normal ovine medial collateral and anterior cruciate ligaments are not accurately recapitulated in scar tissue. *J. Anat.* **200**, 283–294.
- Lotz JC, Colliou OK, Chin JR, Duncan NA, Liebenberg E (1998) Compression-induced degeneration of the intervertebral disc: an in vivo mouse model and finite-element study. *Spine* **23**, 2493–2506.
- Marchand F, Ahmed AM (1990) Investigation of the laminate structure of lumbar disc annulus fibrosus. *Spine* **15**, 402–410.
- Maroudas A, Stockwell RA, Nachemson A, Urban J (1975) Factors involved in the nutrition of the human lumbar intervertebral disc: cellularity and diffusion of glucose in vitro. *J. Anat.* **120**, 113–130.
- Matyas JR (1994) Analysing nuclear shape as a function of relative spatial position in the femoral insertion of the

- medial collateral ligament. *Comput. Meth Programs Biomed.* **44**, 69–77.
- Matyas J, Edwards P, Miniaci A, Shrive N, Wilson J, Bray R, et al.** (1994) Ligament tension affects nuclear shape *in situ*. *An Vitro Study. Conn. Tiss. Res.* **31**, 45–53.
- McNeilly CM, Banes AJ, Benjamin M, Ralphs JR** (1996) Tendon cells *in vivo* form a three dimensional network of cell processes linked by gap junctions [published erratum appears in *J Anat* 1997 April; 190 (Part 3): 477–8]. *J. Anat.* **189**, 593–600.
- Ortolani F, Raspanti M, Franchi M, Marchini M** (1988) Localization of different alcian blue-proteoglycan particles in the intervertebral disc. *Basic Appl. Histochem.* **32**, 443–453.
- Oshima H, Ishihara H, Urban JP, Tsuji H** (1993) The use of coccygeal discs to study intervertebral disc metabolism. *J. Orthop. Res.* **11**, 332–338.
- Postacchini F, Bellocchi M, Massobrio M** (1984) Morphologic changes in annulus fibrosus during aging. An ultrastructural study in rats. *Spine* **9**, 596–603.
- Quist AP, Rhee SK, Lin H, Lal R** (2000) Physiological role of gap-junctional hemichannels. Extracellular calcium-dependent isosmotic volume regulation. *J. Cell Biol.* **148**, 1063–1074.
- Ralphs JR, Benjamin M, Thornett A** (1991) Cell and matrix biology of the suprapatella in the rat: a structural and immunocytochemical study of fibrocartilage in a tendon subject to compression. *Anat. Rec.* **231**, 167–177.
- Ralphs JR, Benjamin M, Waggett AD, Russell DC, Messner K, Gao J** (1998) Regional differences in cell shape and gap junction expression in rat Achilles tendon: relation to fibrocartilage differentiation. *J. Anat.* **193**, 215–222.
- Ralphs JR, Waggett AD, Benjamin M** (2002) Actin stress fibres and cell-cell adhesion molecules in tendons: organisation *in vivo* and response to mechanical loading of tendon cells *in vitro*. *Matrix Biol.* **21**, 67–74.
- Shah JS, Hampson WG, Jayson MI** (1978) The distribution of surface strain in the cadaveric lumbar spine. *J. Bone Joint Surg. Br.* **60-B**, 246–251.
- Shirazi-Adl SA, Shrivastava SC, Ahmed AM** (1984) Stress analysis of the lumbar disc-body unit in compression. A three-dimensional nonlinear finite element study. *Spine* **9**, 120–134.